ORGANIC CHEMISTRY

FRONTIERS

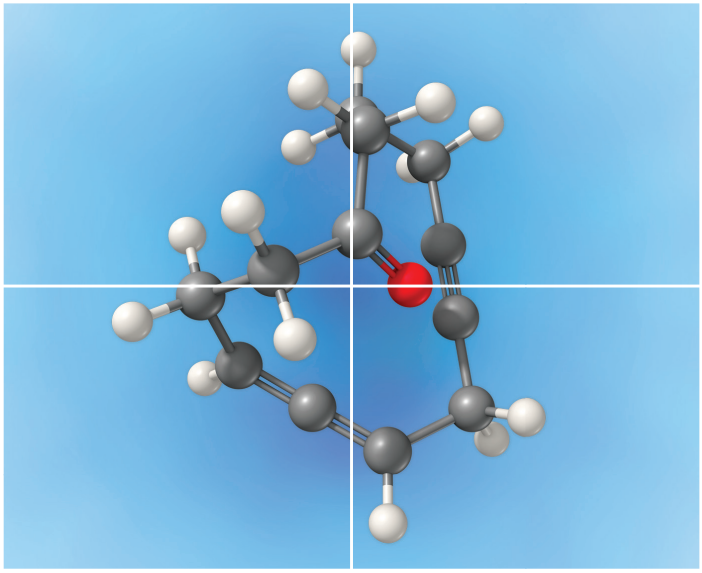

Accepted Manuscript

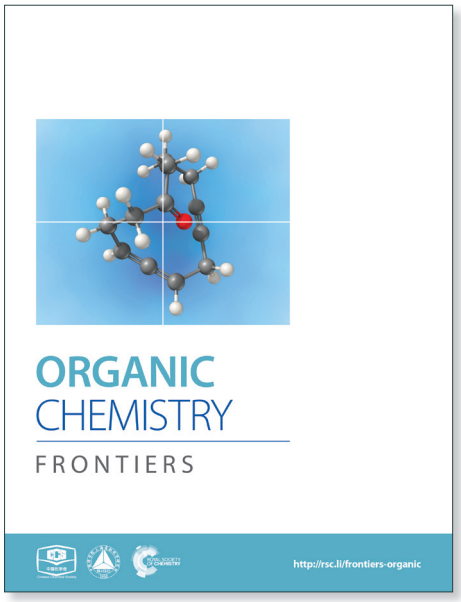

This is an *Accepted Manuscript*, which has been through the Royal Society of Chemistry peer review process and has been accepted for publication.

Accepted Manuscripts are published online shortly after acceptance, before technical editing, formatting and proof reading. Using this free service, authors can make their results available to the community, in citable form, before we publish the edited article. We will replace this *Accepted Manuscript* with the edited and formatted *Advance Article* as soon as it is available.

You can find more information about *Accepted Manuscripts* in the **Information for Authors**.

Please note that technical editing may introduce minor changes to the text and/or graphics, which may alter content. The journal's standard **Terms & Conditions** and the **Ethical guidelines** still apply. In no event shall the Royal Society of Chemistry be held responsible for any errors or omissions in this *Accepted Manuscript* or any consequences arising from the use of any information it contains.

Journal Name

RSCPublishing

ARTICLE

Cite this: DOI: 10.1039/x0xx00000x

Received 00th January 2014,
Accepted 00th January 2014

DOI: 10.1039/x0xx00000x

www.rsc.org/

Understanding the Reaction Mechanisms of Pd-Catalysed Oxidation of Alcohols and Domino Oxidation-Arylation Reactions Using Phenyl Chloride as Oxidant†

Yang Li and Zhenyang Lin*

Density functional theory calculations were carried out to study the Pd-catalysed oxidation reactions of alcohols using phenyl chloride as oxidant. Our calculations supported that the mechanism mainly involves oxidative addition, β-hydride elimination, reductive elimination, and finally ligand substitution. Through our calculations, we have explained why oxidation of secondary alcohol was experimentally observed but not that of primary alcohol. The oxidation products (ketones) of secondary alcohols bind much more weakly than the oxidation products (aldehydes) of primary alcohols, contributing to the reactivity difference. The mechanism of the Pd-catalysed domino oxidation-arylation reactions of secondary alcohols was also studied. We have explained the experimental observation that α-arylation of the oxidation products (ketones) of secondary alcohols occurs only when the temperature was raised to 80 ℃ from below 40 ℃.

Introduction

Transition metal catalysed oxidation of alcohols to carbonyl compounds, which is a fundamental reaction in organic chemistry, has attracted considerable interest over the past years.[1] Examples of transition metals used in these oxidation reactions include iridium,[2] ruthenium,[3] gold,[4] copper,[5] manganese,[6] iron,[7] and palladium.[8] Of these reported oxidation reactions, catalysts based on palladium were particularly attractive and the scope of the related reactions was extensively examined. Ebner *et al.* found that palladium complexes are capable of catalysing enantioselective oxidation of chiral secondary alcohols.[9] Iwasawa *et al.* reported Pd-catalysed aerobic oxidation of alcohols under an air atmosphere in the presence of substituted pyridines.[10]

Development of catalyst systems that can control the ability to selectively oxidize an alcohol in the presence of other groups susceptible to oxidation has been identified as one of the key challenges in alcohol oxidations.[11] In 2009, Navarro *et al.* found that NHC-Pd complexes were able to catalyse oxidation of secondary alcohols at mild temperatures when phenyl chloride was used as oxidant (eq 1). Interestingly, the NHC-Pd complexes did not catalyse the oxidation of primary alcohols at the same reaction condition. Although a reaction mechanism involving oxidative addition, β-hydride elimination, and reductive elimination has been proposed, it cannot account for the experimental observation that secondary alcohols are far more reactive than primary alcohols.[12] On the basis of their work, the same research group reported in 2011 the domino oxidation-arylation reactions of secondary alcohols to produce α-arylated products under the same NHC-Pd catalytic system but at a higher temperature (80 ℃) and in the presence of 2.1 equivalent of the oxidant phenyl chloride (eq 2).[13]

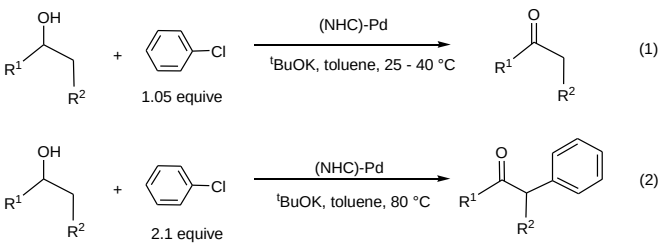

Up to date, theoretical studies on metal-catalysed oxidation of alcohols are limited. Baerends *et al.* theoretically investigated the aerobic oxidation of primary alcohols to aldehydes, using $[Cu(bipy)]^{2+}$, the TEMPO radical, and a strong base as the catalytic system. The most important conclusion of this work is that oxidation of alcohols to aldehydes takes place by electrophilic attack of uncoordinated $TEMPO^{+}$ on one C-H(α) bond of a primary alcohol.[14] Goddard *et al.* theoretically studied the reactivity of $(NHC)Pd(OAc)_2$ and emphasized the role played by the strong trans influence ligand NHC. They found that β-hydride elimination, in which the β-hydrogen of a palladium-bound alkoxide was transferred directly to the free oxygen of the bound carboxylate, provides the lowest-energy route.[15]

*Department of Chemistry, The Hong Kong University of Science and Technology, Clear Water Bay, Kowloon, Hong Kong (China)
Fax: (+852) 2358 1594
E-mail: chzlin@ust.hk

† Electronic supplementary information (ESI) available. See DOI: 10.1039/xxxxxxxxxx

In this work, with the aid of DFT calculations, we will investigate the reactivity difference between primary and secondary alcohols in the Pd-catalysed oxidation reactions (eq 1) by studying the detailed reaction mechanisms. We hope to understand the factors affecting the reactivity difference. We will also study the mechanism related to the Pd-catalysed domino oxidation-arylation reaction shown in eq 2 and understand how higher temperature promotes the α-arylation immediately after the alcohol oxidation. Understanding of the reaction mechanism is expected to lead to more efficient synthetic strategies and more efficient catalysts for oxidation of alcohols to aldehydes or ketones.

Worth mentioning here is that in recent years, environment-friendly alcohol dehydrogenation that does not require an oxidant has been developed to synthesize amides and pyrroles.[16] Wang *et al*. investigated the mechanism of Ru-catalysed reactions of amines with primary alcohols to produce amides.[17] In these reactions, the dehydrogenation reactions normally proceed via the bifunctional double hydrogen transfer mechanism rather than the β-H elimination mechanism.

Computational Details

Full geometry optimizations have been performed at the Becke3LYP (B3LYP) level of the density functional theory.[16] The effective core potentials (ECPs) of Hay and Wadt with a double-ζ valence basis set (LanL2DZ)[18] were used to describe Pd, Cl and K. Polarization functions were added for Pd (ζ_f = 1.47), Cl (ζ_d = 0.64) and K (ζ_d = 1.00).[19] The 6-31G(d) basis set was used for all the other atoms. Frequency calculations were carried out to confirm the characteristics of all of the optimized structures as minima or transition states. Calculations of intrinsic reaction coordinates (IRC)[20] were also performed to confirm that transition states connect two relevant minima. To obtain free energies in solution, the solvation-corrected relative free energies were calculated in Gaussian 09[22] using the M06 DFT functional[23] with the universal solvation model (SMD).[24] Such an approach to obtain the solvation-corrected relative free energies has been popularly used recently in a number of theoretical studies.[25] Toluene was employed as the solvent (according to the reaction conditions).

To reduce the computational cost, we used 1,3-dimethylimidazol-2-ylidine as the model NHC ligand, in which the substituents at N in the experimentally used NHC ligand [(IPr = 1,3-bis-(2,6-diisopropylphenyl)imidazol-2-ylidene)] were replaced by CH_3. Our early work established the validity of using 1,3-dimethylimidazol-2-ylidine as a model for IPr.[26] To provide further support for use of the model NHC ligand, we also calculated the reaction free energies for **1E** + $PhCH_2OH$ → **1A** + PhCHO and **2E** + PhEtCHOH → **2A** + PhEtCO, which are important to our conclusions, with the full NHC ligand used in the experimental reactions. The results show that with the model NHC ligand the reaction free energies are 8.8 and 3.2 kcal/mol (Figures 1 and 3). With the full NHC model, the reaction free energies are 8.7 and 3.9 kcal/mol. We also calculated the free energy changes for **1A** + PhCl → $\mathbf{1TS_{(A-B)}}$ and **2A** + PhCl → $\mathbf{2TS_{(A-B)}}$ with the full NHC ligand. The free energy changes were calculated to be 17.0 and 17.7 kcal/mol (Figures S1 and S2), compared with 20.6 and 20.8 kcal/mol from the model NHC results. Additional comments on the relative barriers using different models are given in the Electronic Supplementary Information.

Results and Discussion

General Mechanism of the Pd-catalysed Oxidation Reactions of Alcohols. As mentioned in the Introduction, reaction mechanism proposed for the Pd-catalysed oxidation reactions of alcohols involves oxidative addition, β-hydride elimination, and reductive elimination. Based on our calculation results, a version of the proposal providing all the relevant details regarding the nature of the species involved is given in Scheme 1. An alcohol molecule first coordinates to the Pd centre to form the two-coordinate active species LPd(0)(alcohol) **A**, which is a 14e Pd(0) complex. 14e Pd(0) complexes are normally considered as the active species for oxidation addition of aryl halides.[27] We consider the two-coordinate active species **A** containing an alcohol molecule, instead of a phenyl chloride as a ligand of the starting species because an alcohol molecule is expected to be more strongly coordinating.

Oxidative addition of phenyl chloride to the complex **A** gives a four-coordinate, square planar Pd(II) complex (**B**).[28] The complex **B** reacts with ^{t}BuOK to give ^{t}BuOH, KCl and the intermediate **C** containing an agostic interaction. The intermediate **C** then undergoes β-hydride elimination to give the complex **D**, which is a precursor complex ready to undergo reductive elimination to give the co-product benzene molecule, and the complex **E** in which the carbonyl product molecule acts as a ligand. Finally, a ligand substitution of substrate (alcohol) for product (aldehyde/ketone) occurs to regenerate the active species **A** and complete the catalytic cycle.

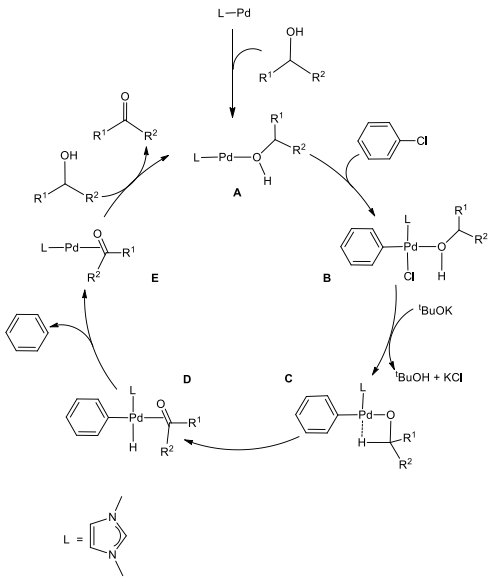

Scheme 1. The proposed mechanism of the Pd-catalysed oxidation reactions of alcohols.

Oxidation of Primary Alcohols. Figure 1 shows the energy profile calculated for the Pd-catalysed oxidation reaction of $PhCH_2OH$, a primary alcohol, ($PhCH_2OH$ → PhCHO) on the basis of the reaction mechanism illustrated in Scheme 1. In Figure 1, oxidative addition of phenyl chloride to the two-coordinate complex active species **1A** occurs as the first step via the transition state $\mathbf{1TS_{(A-B)}}$ to give the square-planar Pd(II) intermediate **1B** with a barrier of 20.6 kcal/mol. Here, **1A** + PhCl, instead of the van der Waals complex of the two, were set as the energy reference point, considering the entropy contribution. In fact, the van der Waals complex of the two is lying higher in free energy than **1A** + PhCl. Then the base ^{t}BuOK neutralizes HCl eliminated from the intemediate **1B** to give ^{t}BuOH + KCl and the intermediate **1C** which contains an agostic interaction. Next, β-hydride elimination gives the hydride intermediate **1D**. Then, reductive elimination takes place to release a benzene molecule and form the intermediate **1E**. In the intermediate **1E**, the carbonyl product molecule is coordinated to the metal centre as a

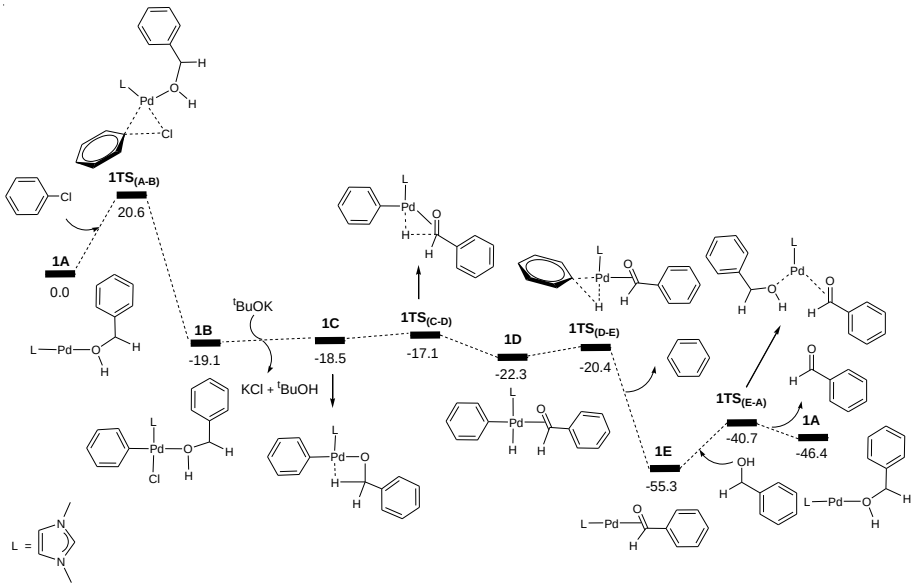

Figure 1. Energy profile calculated for the Pd-catalysed oxidation of $PhCH_2OH$ ($PhCH_2OH$ + PhCl + ^tBuOK → PhCHO + PhH + ^tBuOH + KCl). The relative free energies are given in kcal/mol.

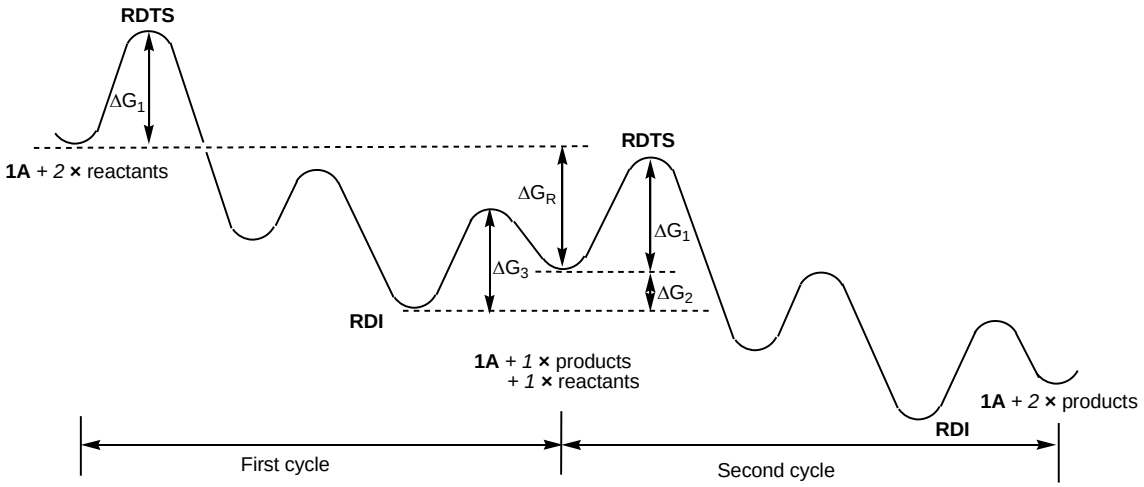

Figure 2. Schematic illustration of the energy profile given in Figure 1, which includes the energy profile for an additional catalytic cycle.

ligand through an η^2-coordination of the C=O bond. We can see that once the intermediate **1B** is formed, the steps followed leading to **1E** are all very facile. Finally, a ligand substitution gives the final aldehyde product PhCHO and regenerates the active species **1A**. Here, **1E** is the resting state of the catalytic cycle on the basis of our theoretical calculations.

The energy profile shown in Figure 1 indicates that the overall reaction is highly exergonic with a reaction free energy of -46.4 kcal/mol ($PhCH_2OH$ + PhCl + ^tBuOK → PhCHO + PhH + ^tBuOH + KCl). The highest energy structure in the energy profile corresponds to the transition state **$1TS_{(A-B)}$** which lies 20.6 kcal/mol higher in energy than the energy reference point (**1A** + $PhCH_2OH$ + PhCl + ^tBuOK). From the energy profile shown in Figure 1, one may rush to conclude that the overall barrier for the catalytic reaction corresponds to the barrier calculated for the oxidative addition of PhCl to **1A**, which is 20.6 kcal/mol. This is not the case because the lowest energy point in the catalytic cycle corresponds to the intermediate **1E**, not the end point of the catalytic cycle. We can see that **1E** + $PhCH_2OH$ is more stable than **1A** + PhCHO by 8.9 kcal/mol (Figure 1). In fact, the overall barrier for the catalytic reaction should be 20.6 + 8.9 = 29.5 (kcal/mol) according the energetic span model developed by Kozuch *et al.*[29]

To further elaborate the application of the energetic span model in the case here, we depicted the schematic energy profile diagram in Figure 2 by extending the energy profile for an additional catalytic cycle. In Figure 2, **RDTS** and **RDI** stand for rate-determining transition state and intermediate, respectively. ΔG_R is the reaction free energy for the catalytic reaction under consideration. From Figure 2, we can also view the first **RDI** to the second **RDI** as a catalytic cycle. In this view, we can easily come to the conclusion that the overall barrier is $\Delta G_1 + \Delta G_2$, not a simple addition of the two relevant barriers ($\Delta G_1 + \Delta G_3$). In Figure 1, we have that ΔG_1 = 20.6 kcal/mol and ΔG_2 = 8.9 kcal/mol.

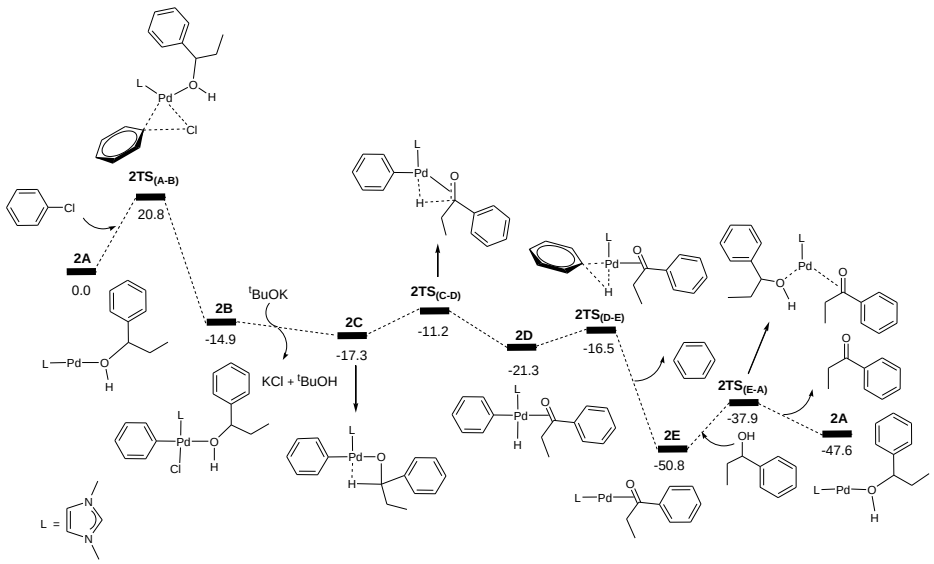

Figure 3. Energy profile calculated for the Pd-catalysed oxidation of PhEtCHOH (PhEtCHOH + PhCl + ^{t}BuOK → PhEtCO + PhH + ^{t}BuOH + KCl). The relative free energies are given in kcal/mol.

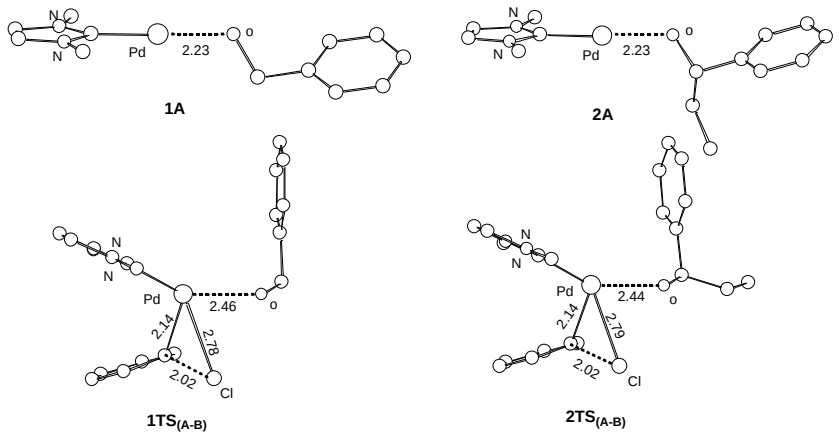

Figure 4. Selected bond distances (Å) calculated for the active species **1A** and **2A** and the oxidative addition transition states **1TS(A-B)** and **2TS(A-B)**. Hydrogen atoms have been omitted for the purpose of clarity.

Oxidation of Secondary Alcohols. For comparison, we also calculated the energy profile for the corresponding catalysed oxidation reaction of the secondary alcohol PhEtCHOH (PhEtCHOH → PhEtCO) on the basis of the reaction mechanism shown in Scheme 1. Figure 3 shows the calculated energy profile. From Figure 3, we see that the energy profile is very similar to that calculated for the catalysed oxidation of $PhCH_2OH$ shown in Figure 1. The transition state **2TS$_{(A-B)}$** corresponds to the highest energy structure in the energy profile, which lies 20.8 kcal/mol above the energy reference point. **2TS$_{(A-B)}$** is in fact the transition state for the oxidative addition of PhCl to **2A**. Clearly, the barrier (20.8 kcal/mol) calculated for the oxidative addition of PhCl to **2A** is approximately the same as that (20.6 kcal/mol, Figure 1) calculated for the oxidative addition of PhCl to **1A**.

Similar to what we found for the reaction of the primary alcohol $PhCH_2OH$, the intermediate **2E** having the product molecule PhEtCO as a ligand also corresponds to the lowest energy point in the energy profile. However, **2E** + PhEtCHOH is more stable than **2A** + PhEtCO by 3.2 kcal/mol only. In the reaction of the primary alcohol $PhCH_2OH$, **1E** + $PhCH_2OH$ is more stable than **1A** + PhCHO by 8.9 kcal/mol. Thus, the overall barrier for the catalytic reaction of the secondary alcohol PhEtCHOH is 20.8 + 3.2 = 24.0 (kcal/mol). The overall reaction (PhEtCHOH + PhCl + ^{t}BuOK → PhEtCO + PhH + ^{t}BuOH + KCl) is exergonic with a reaction free energy of -47.6 kcal/mol.

Reactivity Difference between Primary and Secondary Alcohols. The calculation results described above indicate that the Pd-catalysed oxidation reaction of the secondary alcohol PhEtCHOH is kinetically more favorable than that of the primary alcohol $PhCH_2OH$ by 5.5 kcal/mol. The barrier difference (5.5 kcal/mol) can give a multiplicative difference of about 10^5 in the reaction rate if we assume an Arrhenius expression for the rate constant and similar preexponential factors. Experimentally, oxidation reaction of the secondary alcohol PhEtCHOH was carried out at 25 ℃ and took 11 hours to achieve a yield of 91%.[13] Given the difference in the reaction rate, it is expected that oxidation reaction of the corresponding primary alcohol $PhCH_2OH$ was not observed experimentally.

Analysis given above indicates that the overall barrier for the catalysed oxidation of a given alcohol substrate molecule is the sum

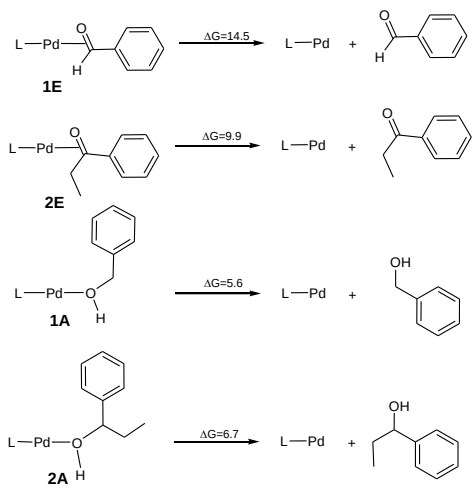

Scheme 2. The binding energies of the alcohol substrate molecules and the corresponding aldehyde/ketone product molecules with the Pd(0) metal centre.

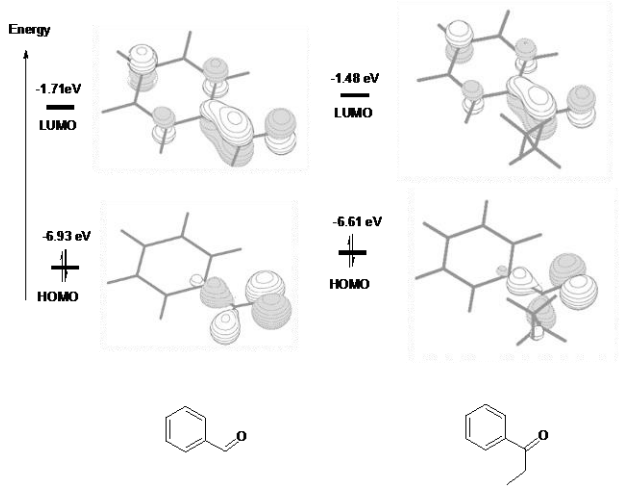

Figure 5. The HOMO and LUMO calculated for PhCHO and PhEtCO. The orbital energies are given in eV.

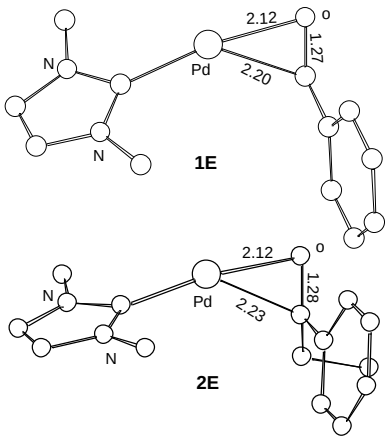

Figure 6. Selected bond distances (Å) calculated for the ligand substitution intermediates **1E** and **2E**. Hydrogen atoms have been omitted for the purpose of clarity.

of (1) the barrier (ΔG_1) for oxidative addition of PhCl to the active species LPd(0)(substrate) (**1A** or **2A**) and (2) the reaction free energy (ΔG_2) for the ligand substitution of an alcohol substrate molecule for an aldehyde or ketone product molecule in LPd(0)(product) to regenerate the active species.

Our calculations show that the barriers (ΔG_1) for the oxidative additions of phenyl chloride to **1A** and **2A** are approximately the same. Examining the structures of **1A**, **2A** and the corresponding oxidative addition transition states $\mathbf{1TS_{(A-B)}}$ and $\mathbf{2TS_{(A-B)}}$ (Figure 4), we see that the optimized structures of **1A** and **2A** as well as $\mathbf{1TS_{(A-B)}}$ and $\mathbf{2TS_{(A-B)}}$ are similar to each other. The results are consistent with that the approximately same barriers were calculated for the two oxidative additions.

As discussed above, the ligand substitution of an alcohol substrate molecule for an aldehyde or a ketone product molecule is another step contributed to the overall barrier. The energetics (ΔG_2) associated with the ligand substitution step reflects how relatively easy an aldehyde or a ketone product molecule, once it is formed, is released from the catalyst to which it is coordinated. The calculation results show that **1E** + $PhCH_2OH$ → **1A** + PhCHO is more endergonic than **2E** + PhEtCHOH → **2A** + PhEtCO by 5.5 kcal/mol. Here, we can see that it is the difference in (ΔG_2) that contributes to the significant reactivity difference of the two substrate molecules.

Scheme 2 compares the binding energies of the alcohol substrate molecules and the corresponding aldehyde/ketone product molecules with the Pd(0) metal centre. A relatively small difference in the binding energy was calculated between the two alcohol substrate molecules. However, a noticeably significant difference in the binding energy can be found between the two product molecules. Clearly, the product molecule PhCHO derived from the former alcohol substrate molecule binds much more strongly to the Pd(0) metal centre than the product molecule PhEtCO derived from the latter alcohol substrate molecule. The stronger η^2-binding of PhCHO versus PhEtCO with Pd(0) can be attributed to both steric and electronic effects. PhCHO is less sterically hindered than PhEtCO when it is η^2-coodinated to the metal centre. Electronically, PhCHO has a lower lying C=O π^* orbital when compared with PhEtCO (Figure 5), giving rise to greater Pd(0)-to-CO(π^*) back-bonding interaction. In the calculated structures shown in Figure 6, **1E** gives shorter Pd-C(O) distance than **2E** does.

$[LPd(OtBu)]^-$ as the active species. In the presence of ^{t}BuOK, one might argue that the anionic species $[LPd(O^tBu)]^-$, instead of LPd(0)(alcohol) **A**, acted as the active species for the catalytic process. Considering this anionic species as the active species, we also calculated the energy profile for the catalysed oxidation reaction of the primary alcohol $PhCH_2OH$. The detailed energy profile (Figure S3) and the mechanistic cycle (Scheme S1) which is very similar to Scheme 1 except the active species are given in the Electronic Supplementary Information. Interestingly, the overall reaction barrier was found to be only 17.3 kcal/mol. With such a small overall reaction barrier, one would expect that the reaction could occur easily and quickly. However, the experimental finding is that the reaction occurs at the elevated temperature 25 - 40 ^oC and takes hours to complete. Therefore, in the actual reaction, the anionic species $[LPd(O^tBu)]^-$ is unlikely to be involved as the active species in the catalytic cycle.

A plausible explanation for the anionic species $[LPd(O^tBu)]^-$ not being involved as the active species is given as follows. Experimentally, tertbutoxide has very poor solubility in toluene, which is the solvent used in the reactions. Alcohol and the catalyst are much more soluble in toluene than tertbutoxide. Therefore, it is reasonable to assume that formation of LPd(0)(alcohol) is much faster than that of $[LPd(O^tBu)]^-$.

With LPd(0)(alcohol) as the active species, oxidative addition of PhCl has a reasonably small barrier and is expected to a fast step also. Once LPd(II)Ph(Cl)(alcohol) is formed from the oxidative addition, the coordinated alcohol in this Pd(II) complex is much more acidic (when compared with the coordinated alcohol in LPd(0)(alcohol)) and easily deprotonated by tertbutoxide as proposed in Scheme 1.

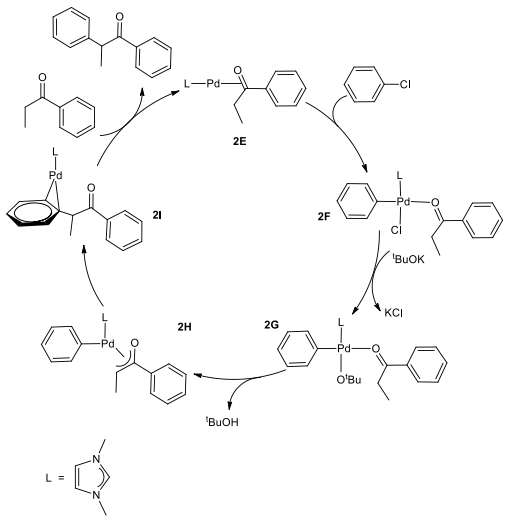

Scheme 3. The proposed mechanism of the Pd-catalysed α-arylation reaction of PhEtCO.

Decarbonylation of LPd(0)(PhCHO) (1E). Another possible reason for the oxidation reaction of primary alcohol $PhCH_2OH$ not being observed could be due to decarbonylation of LPd(0)(PhCHO) (**1E**) via C-H oxidative addition. We studied this possibility (see ESI for the calculated energy profile). From **1E**, oxidative addition of the C-H bond to the Pd centre occurs to give a hydride intermediate. Then α-phenyl migration to the metal centre gives a four-coordinate complex (LPd(II)H(CO)Ph), in which CO is a ligand. Finally, the reductive elimination takes place to release a benzene molecule and form a two-coordinate complex containing the NHC ligand and CO. An overall free energy barrier of 41.3 kcal/mol was calculated for the α-phenyl migration. With such an inaccessibly high barrier, we cannot argue that decarbonylation is responsible for the oxidation reaction of primary alcohol $PhCH_2OH$ not being observed.

Mechanism of the Pd-catalysed Domino Oxidation-arylation of Secondary Alcohols. Now we come to understand the Pd-catalysed domino oxidation-arylation reactions of secondary alcohols shown in eq 2 in which α-arylated products were produced when two equivalents of the oxidant phenyl chloride were used in the reaction. Here, we can reasonably hypothesize that the secondary alcohols were first oxidized to their corresponding ketones and then further reacted with the second equivalent of the oxidant phenyl chloride at a higher temperature to finally produce the α-arylated products. Indeed, experimental evidence supports this hypothesis. Experimentally, α-arylated products were produced when ketones derived from eq 1 were allowed to react with phenyl chloride at 80 ℃ under the same catalytic system.[13] In other words, the key to understanding the reaction mechanism for eq 2 is to understand how a ketone molecule reacts with phenyl chloride.

Here, we use the product molecule PhEtCO (discussed above) as a substrate ketone to react with phenyl chloride (the α-arylation reaction). Figure 3 shows that the last step **2E** + PhEtCHOH → **2A** + PhEtCO, which is a ligand substitution process, is reversible. Therefore, instead of undergoing the ligand substitution, **2E** can further react with PhCl via oxidative addition to give a four-coordinate, square planar Pd(II) species **2F** (Scheme 3). From the species **2F**, a ligand substitution of $^tBuO^-$ for Cl^- gives the intermediate **2G**. Subsequently, deprotonation at the α-carbon by the $^tBuO^-$ ligand produces the η^3 intermediate **2H** and ^{t}BuOH. Then, reductive elimination in the **2H** takes place to give the intermediate **2I** in which the α-arylated product molecule acts as a ligand. Finally, a ligand substitution of a ketone molecule for the α-arylated product molecule regenerates the active catalytic species **2E** and completes the α-arylation reaction.

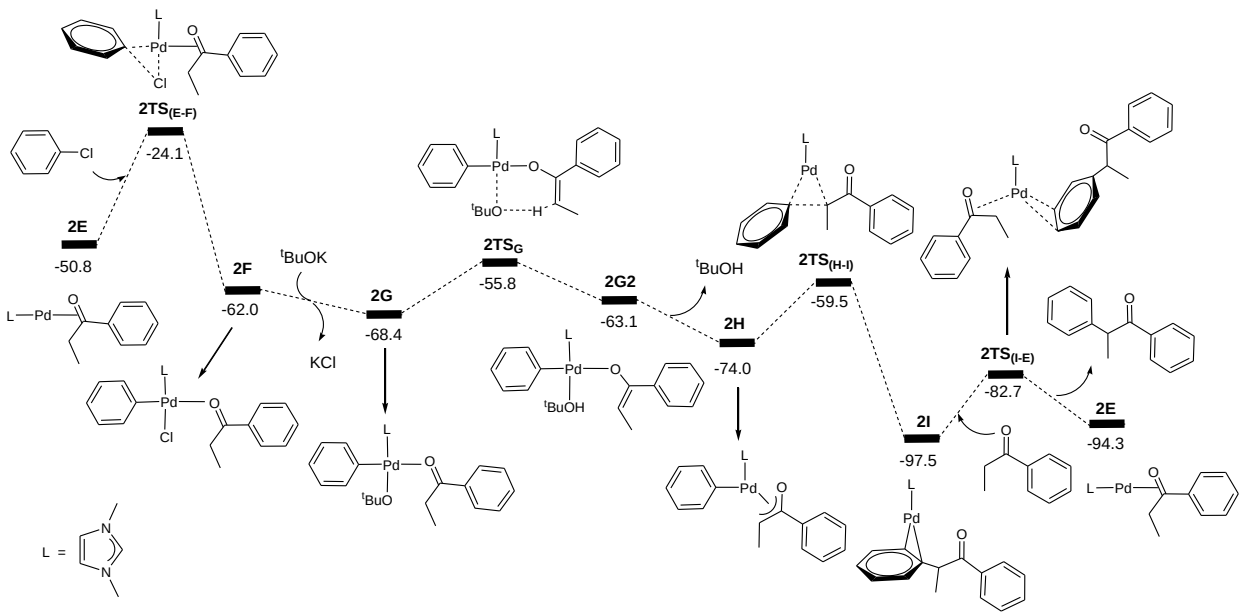

Figure 7. Energy profile calculated for the Pd-catalysed α-arylation reaction of PhEtCO. The relative free energies are given in kcal/mol.

Figure 7 shows the energy profile calculated for the Pd-catalysed α-arylation reaction of PhEtCO based on the mechanism proposed in Scheme 3. The first step is the oxidative addition of phenyl chloride to the two-coordinate complex **2E** to give the intermediate **2F** via the transition state $\mathbf{2TS_{(E\text{-}F)}}$. The free energy barrier calculated for this step is 26.7 kcal/mol. From **2F**, a ligand substitution of $^{t}BuO^{-}$ for Cl^{-} occurs to give the intermediate **2G**, in which the $^{t}BuO^{-}$ ligand coordinates to the metal centre. The deprotonation from **2G** proceeds to **2G2** via the transition state $\mathbf{2TS_{G}}$, which involves migration of one proton at the coordinated-PhEtCO α-carbon to the $^{t}BuO^{-}$ ligand. In the **2G2** intermediate, $^{t}BuOH$ is easily dissociated to form the more stable intermediate **2H**. Reductive elimination in **2H** occurs to give the two-coordinated intermediate **2I** via the transition state $\mathbf{2TS_{(H\text{-}I)}}$, in which the α-arylated product molecule is coordinated as a ligand to the metal centre in an η^2 coordination mode. In the final step, a ligand substitution of PhEtCO for the α-arylation product regenerates the active catalytic species **2E** and completes the α-arylation reaction.

The energy profile shown in Figure 7 indicates that the overall reaction PhEtCO + PhCl + $^{t}BuOK$ → $CH_3CH(Ph)C(O)Ph$ + $^{t}BuOH$ + KCl is exergonic with a reaction free energy of -43.5 kcal/mol. The highest energy structure in the energy profile corresponds to the transition state $\mathbf{2TS_{(E\text{-}F)}}$ which lies 26.7 kcal/mol higher in energy than the energy reference point (**2E** + PhEtCO + PhCl + $^{t}BuOK$). The lowest energy structure corresponds to the intermediate **2I**. **2I** + PhEtCO is more stable than **2E** + $CH_3CH(Ph)C(O)Ph$ by 3.2 kcal/mol. As mentioned above, the overall barrier for the α-arylation reaction is 29.9 kcal/mol, the sum of 26.7 kcal/mol and 3.2 kcal/mol according to what we discussed above (Figure 2).

The calculation results indicate that the α-arylation of the oxidation product PhEtCO has a higher overall free energy barrier than the oxidation of PhEtCHOH. Therefore, it is expected that at a lower temperature, the reaction stops at the oxidation reaction while at a higher temperature the reaction can continue to give the α-arylated product. These results well explain that the oxidation reaction occurs below 40 ℃ and further reaction (α-arylation reaction) of the oxidation product occurs when the temperature was raised to 80 ℃. We would like to point out here that the ability of a ketone being enolized (formation of **2H**), but not benzaldehyde, contributes to the fact that the secondary alcohols can further react with one more equivalent of PhCl leading to α-arylation.

Conclusion

The Pd-catalysed oxidation reactions of primary and secondary alcohols to the corresponding aldehydes and ketones, respectively, by phenyl chloride have been investigated with the aid of DFT calculations. The results of the calculations support that the mechanism mainly involves oxidative addition, β-hydride elimination, reductive elimination, and finally ligand substitution.

Experimentally, selective oxidation of secondary alcohols versus primary alcohols has been observed. Consistent with this experimental observation, the oxidation reaction of the secondary alcohol PhEtCHOH was calculated to be kinetically more favorable than that of the primary alcohol $PhCH_2OH$. Our detailed mechanistic analysis indicates that the overall reaction barrier for the oxidation of a given alcohol substrate molecule is the sum of (1) the barrier for oxidative addition of phenyl chloride to the active species LPd(0)(alcohol) and (2) the reaction free energy for the ligand substitution of the alcohol substrate molecule for the aldehyde or ketone product molecule in LPd(0)(aldehyde) or LPd(0)(ketone) to regenerate the active species LPd(0)(alcohol). We found that a ketone product molecule binds much more weakly to the Pd(0) metal centre than an aldehyde product molecule, explaining that oxidation of secondary alcohols, but not primary alcohols, occurs under the catalytic condition.

The Pd-catalysed domino oxidation-arylation reactions of secondary alcohols have also been investigated. Our calculation results support that the secondary alcohols were first oxidized by phenyl chloride to their corresponding ketones according the mechanism summarized above and then further reacted with the second equivalent of the oxidant phenyl chloride at a higher temperature to finally produce the α-arylated products. In the α-arylation reaction of the ketone product molecule, we have established that the mechanism involves (1) oxidative addition of PhCl to LPd(0)(ketone), (2) ligand substitution of $^{t}BuO^{-}$ for Cl^{-}, (3) deprotonation of an α-H of the coordinated ketone molecule by the $^{t}BuO^{-}$ ligand, and (4) reductive elimination to give a species which contains the α-arylated product molecule as a ligand, (5) finally a ligand substitution of a ketone molecule for the α-arylated product molecule to regenerate the active species LPd(0)(ketone). The overall barrier calculated for the α-arylation of the oxidation product PhEtCO was found to be higher than the oxidation of the secondary alcohol PhEtCHOH. These results explain the experimental observation that α-ketone arylation occurs when the temperature was raised to 80 ℃ from below 40 ℃.

As a final note to readers, we would like to point out that the conclusions summarized above are based on the assumption that LPd(0)(alcohol) is the active species for the catalytic cycle. In the presence of $^{t}BuOK$, one would expect that the anionic species $[LPd(0)(O^{t}Bu)]^{-}$ is likely the active species. However, our calculations show that the anionic species $[LPd(0)(O^{t}Bu)]^{-}$ gives an overall reaction barrier of 17.3 kcal/mol for the catalysed oxidation of $PhCH_2OH$, which is too small to account for the oxidation reactions observed experimentally (slow and with elevated temperature). We argue that the poor solubility of the tertbutoxide and the solvent used (toluene) prevents the fast formation of the anionic species. We also examined whether decarbonylation is responsible for the oxidation reaction of primary alcohol $PhCH_2OH$ not being observed. Our calculation results do not support this. We hope that this work will invite more research on these reactions to gain more insights into the reaction mechanism.

Acknowledgements

This work was supported by the Research Grants Council of Hong Kong (HKUST603711, HKUST603313 and CUHK7/CRF/12G).

Notes and references

1 a) Y. M. A. Yamada, C. K. Jin, Y. Uozumi, *Org. Lett.*, **2010**, *12*, 4540; b) F. Hanasaka, K. Fujita, R. Yamaguchi, *Organometallics* **2004**, 23, 1490; c) A. S. Guram, X. Bei, H. W. Turner, *Org. Lett*. **2003**, 5, 2485.

2 a) A. V. Polukeev, P. V. Petrovskii, A. S. Peregudov, M. G. Ezernitskaya, A. A. Koridze, *Organometallics* **2013**, 32, 1000; b) R. Kawahara, K. Fujita, R. Yamaguchi, *J. Am. Chem. Soc*. **2012**, 134, 3643; c) B. Jiang, Y. Feng, E. A. Ison, *J. Am. Chem. Soc*. **2008**, 130, 14462.

3 a) S. Manzini, C. A. Urbina-Blanco, S. P. Nolan, *Organometallics* **2013**, 32, 660; b) A. J. A. Watson, A. C. Maxwell, J. M. J. Williams, *Org. Lett*. **2010**, 12, 3856; c) B.-Z. Zhan, M. A. White, T.-K. Sham, J. A. Pincock, R. J. Doucet, K. V. R. Rao, K. N. Robertson, T. S. Cameron, *J. Am. Chem. Soc*. **2003**, 125, 2195.

4 B. Guan, D. Xing, G. Cai, X. Wan, N. Yu, Z. Fang, L. Yang, Z. Shi, *J. Am. Chem. Soc*. **2005**, 127, 18004.
5 a) X. Liu, Q. Xia, Y. Zhang, C. Chen, W. Chen, *J. Org. Chem*. **2013**, 78, 8531; b) I. E. Markó, A. Gautier, R. Dumeunier, K. Doda, F. Philippart, S. M. Brown, C. J. Urch, *Angew. Chem. Int. Ed*. **2004**, 43, 1588.
6 M. K. Brown, M. M. Blewett, J. R. Colombe, E. J. Corey. *J. Am. Chem. Soc*. **2010**, 132, 11165.
7 J. Liu, S. Ma, *Org. Lett*. **2013**, 15, 5150.
8 a) K. Mori, T. Hara, T. Mizugaki, K. Ebitani, K. Kaneda, *J. Am. Chem. Soc*. **2004**, 126, 10657; b) J. A. Mueller, D. R. Jensen, M. S. Sigman, *J. Am. Chem. Soc*. **2002**, 124, 8202.
9 D. C. Ebner, R. M. Trend, C. Genet, M. J. McGrath, P. O'Brien, B. M. Stoltz, *Angew. Chem. Int. Ed*. **2008**, 47, 6367.
10 T. Iwasawa, M. Tokunaga, Y. Obora, Y. Tsuji, *J. Am. Chem. Soc*. **2004**, 126, 6554.
11 J. Muzart, *Tetrahedron*. **2003**, 59, 5789.
12 C. Berini, D. F. Brayton, C. Mocka, O. Navarro. *Org. Lett*. **2009**, 11, 4244.
13 B. Landers, C. Berini, C. Wang, O. Navarro. *J. Org. Chem*. **2011**, 76, 1390.
14 C. Michel, P. Belanzoni, P. Gamez, J. Reedijk, E. J. Baerends, *Inorg. Chem*. **2009**, 48, 11909.
15 R. J. Nielsen, W. A. Goddard III, *J. Am. Chem. Soc*. **2006**, 128, 9651.
16 a) C. Gunanathan, Y. Ben-David, D. Milstein, *Science.* **2007**, *317*, 790; b) B. Kang, X. Huang, L. Xie, N. Maulide, J. Am. Chem. Soc. **2013**, *135*, 11704; c) S. Michlik, R. Kempe, *Nature Chemistry*. **2013**, *5*, 140; d) D. Srimani, Y. Ben-David, D. Milstein. *Angew. Chem., Int. Ed*. **2013**, 52, 4012; e) H. Li, X. Wang, F. Huang,G. Lu, J. Jiang, Z. Wang, *Organometallics* **2011**, 30, 5233; f) G. Zeng, S. Li, *Inorg. Chem.*, **2011**, 50, 10572; g) G. B. Hall, R. Kottani, G. A. N. Felton, T. Yamamoto, D. H. Evans, R. S. Glass, D. L. Lichtenberger, S. *J. Am. Chem. Soc.*, **2014**, *136*, 4012.
17 a) C. Song, S. Qu, Y. Tao, Y. Dang, Z. Wang. *ACS Catal.*, **2014**, *4*, 2854; b) H. Li, G. Lu, J. Jiang, F. Huang, Z.Wang, *Organometallics*, **2011**, *30*, 2349.
18 a) P. J. Stephens, F. J. Devlin, C. F. Chaobalowski, M. J. Frisch, *J. Phys. Chem*. **1994**, 98, 11623; b) A. D. Becke, *J. Chem. Phys*. **1993**, 98, 5648; c) B. Miehlich, A. Savin, H. Stoll, H. Preuss, *Chem. Phys. Lett*. **1989**, 157, 200; d) C. Lee, W. Yang, G. Parr, *Phys. Rev. B*. **1988**, 37, 785.
19 a) W. R. Wadt, P. J. Hay, *J. Chem. Phys*. **1985**, 82, 284; b) P. J. Hays, W. R. Wadt, *J. Chem. Phys*. **1985**, 82, 299.
20 a) A. W. Ehlers, M. Böhme, S. Dapprich, A. Gobbi, A. Höllwarth, V. Jonas, K. F. Köhler, R. Stegmenn, G. Frenking, *Chem. Phys. Lett*. **1993**, 208, 111-114; b) A. Höllwarth, M. Böhme, S. Dapprich, A. W. Ehlers, A. Gobbi, V. Jonas, K. F. Köhler, R. Stegmenn, A. Veldkamp, G. Frenking, *Chem. Phys. Lett*. **1993**, 208, 237.
21 a) K. Fukui, *Acc. Chem. Res*. **1981**, 14, 363-375; b) K. Fukui, *J. Phys. Chem*. **1970**, 74, 4161.
22 M. J. Frisch, *et al.* Gaussian 09, revision D. 01; Gaussian, Inc., Pittsburgh, PA, **2009**.
23 a) Y. Zhao, D. G. Truhlar, *Acc. Chem. Res*. **2008**, 41, 157; b) Y. Zhao, D. G. Truhlar, *Theor. Chem. Acc*. **2008**, 120, 215.
24 A. V. Marenich, C. J. Cramer, D. G. Truhlar, *J. Phys. Chem. B* **2009**, 113, 6378.
25 a) F. Liu, R. S. Paton, S. Kim, Y. Liang, K. N. Houk, *J. Am. Chem. Soc*. **2013**, 135, 15642; b) N. Lo, H. Chen, W. Chuang, C. Lu, P. Chen, P. Chen, *J. Phys. Chem. B* **2013**, 117, 13899; c) Y. Li, Z. Lin, *J. Org. Chem*. **2013**, 78, 11357; d) Q. Xu, H. Gao, M. Yousufuddin, D. H. Ess, L. Kürti, *J. Am. Chem. Soc*. **2013**, 135, 14048.
26 a) L. Dang, Z. Lin, T. B. Marder, *Organometallics* **2010**, 29, 917; b) L. Dang, Z. Lin, T. B. Marder, *Chem. Commun*. **2009**, 3987; c) H. T. Zhao, L. Dang, T. B. Marder, Z. Lin, *J. Am. Chem. Soc*. **2008**, 130, 5586; d) L. Dang, H. T. Zhao, Z. Lin, T. B. Marder, *Organometallics* **2008**, 27, 1178; e) H. T. Zhao, Z. Lin, T. X B. Marder, *J. Am. Chem. Soc*. **2006**, 128, 15637.
27 a) A. A. C. Braga, N. H. Morgon, G. Ujaque, F. Maseras, *J. Am. Chem. Soc*. **2005**, 127, 9298; b) R. B. Bedford, C. S. J. Cazin, *Organometallics* **2003**, 22, 987; c) E. Galardon, S. Ramdeehul, J. M. Brown, A. Cowley, K. K. Hii, A. Jutand, *Angew. Chem., Int. Ed*. **2002**, 41, 1760.
28 a) M. García-melchor, A. A. C. Braga, A. Lledós, G. Ujaque, F. Maseras, *Acc. Chem. Res*. **2013**, 46, 2626; b) L. Xue, Z. Lin, *Chem. Soc. Rev*. **2010**, 39, 1692; c) U. Christmann, R. Vilar, *Angew. Chem., Int. Ed*. **2005**, 44, 366; d) G. B. Smith, G. C. Dezeny, D. L. Hughes, A. O. King, T. R. Verhoeven, *J. Org. Chem*. **1994**, 59, 8151.
29 S. Kozuch, S. Shaik, *Acc. Chem. Res*. **2011**, 44, 101.

